ACS APPLIED POLYMER MATERIALS

pubs.acs.org/acsapm Article

pH-Responsive Antibacterial Surfaces Based on Cross-Linked Phosphonium Polymers

Mónica Vásquez Peña, Karen Nygard, Paul J. Ragogna, and Elizabeth R. Gillies*

Cite This: ACS Appl. Polym. Mater. 2024, 6, 6208−6218 Read Online

ACCESS | Metrics & More | Article Recommendations | Supporting Information

ABSTRACT: With growing concerns regarding biofilms and the development of antibiotic resistance, there is significant interest in antibacterial surfaces. Surfaces that can exhibit antibacterial activity in response to stimuli associated with bacteria and biofilm development are particularly attractive as they can mitigate off-target toxicity and minimize antimicrobial resistance. One such stimulus is a local reduction in pH, which is associated with the production of organic acids by bacteria. We describe here coatings composed of phosphonium monomers and pH-sensitive acetal or ketal-containing cross-linkers that are designed to break down and release active phosphonium species at mildly acidic pH. Four styrenic phosphonium monomers were investigated, and the tributyl(4-vinylbenzyl)phosphonium chloride and triphenyl(4-vinylbenzyl)-phosphonium chloride monomers provided coatings with efficient curing, water contact angles of 50−62°, and surface charge densities of >10^{16} cations cm^{-2}. Coatings prepared from these monomers using the acetal cross-linker were very stable at pH 4.5−7.4 over 3 weeks, whereas those containing the ketal cross-linker exhibited pH-dependent degradation, with complete degradation over 1 week at pH 5. At pH 5, the ketal cross-linker coatings were confirmed to release phosphonium species that effectively killed *Escherichia coli* and *Staphylococcous aureus*, whereas the same coatings at pH 7.4 as well as the acetal cross-linker coatings at both pH 5 and 7.4 released minimally active concentrations of species. The effects of the coatings on bacteria seeded directly on the surfaces were also examined, and it was found that while some coatings exhibited modest antibacterial activity at pH 7.4 or with the slowly degrading acetal cross-linker, coatings containing the rapidly degradable ketal cross-linker consistently provided the highest inhibition of bacterial growth at pH 5. These results were confirmed by live/dead staining. Overall, this work indicates the potential of pH-sensitive phosphonium surfaces to provide pH-dependent bacterial killing, which can potentially prevent biofilm development.

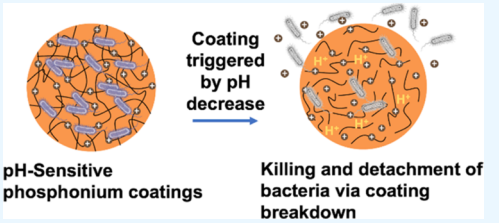

KEYWORDS: *phosphonium, coating, antibacterial, pH-responsive, acetal, ketal, cross-link*

INTRODUCTION

Bacterial contamination of surfaces is a major ongoing challenge, impacting diverse areas such as water quality, food safety, textiles, ventilation, corrosion, and medical or dental implants.[1−5] While planktonic bacteria initially interact with surfaces through reversible interactions, these interactions can become irreversible, leading to the development of a biofilm,[6] a complex assembly of microorganisms enclosed in a matrix of extracellular polymeric substances (EPS). Biofilms are particularly difficult to eradicate because the EPS act as a protective barrier that reduces the permeability of antibacterial agents (e.g., antibiotics), thus accelerating resistance development due to bacterial communication through quorum sensing or horizontal gene transfer.[7,8] Furthermore, in the context of implants, biofilms serve as a barrier to the clearance of the infection by the immune system.[9]

Given that the initial step for biofilm formation is bacterial attachment to the surface, there has been substantial interest in the development of surfaces and coatings that can either reduce the adhesion of and/or kill bacteria.[10−13] To reduce adhesion, antifouling surfaces such as those coated with poly(ethylene glycol)[14] or zwitterionic polymers[15] have been developed. The incorporation of antibacterial agents such as metals (silver or copper),[16,17] nitric oxide,[18] or antibiotics[19,20] that can be gradually released over time has also been investigated. Surfaces with covalently bound cations such as ammoniums or phosphoniums have also been demonstrated to kill bacteria through the disruption of anionic bacterial cell membranes, a mechanism that is thought to be less conducive to the development of resistance, compared to that of antibiotics.[21−25] Coatings that possess more than one of the above features have also been studied.[26−28]

Stimuli-responsive antibacterial coatings have been garnering increasing attention as the approach of releasing antibacterial agents on demand can potentially enhance their efficacy and minimize the generation of drug-resistant bacteria.[29−33] Various stimuli have been investigated. For example, building

Received: January 18, 2024
Revised: April 24, 2024
Accepted: May 7, 2024
Published: May 16, 2024

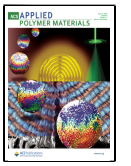

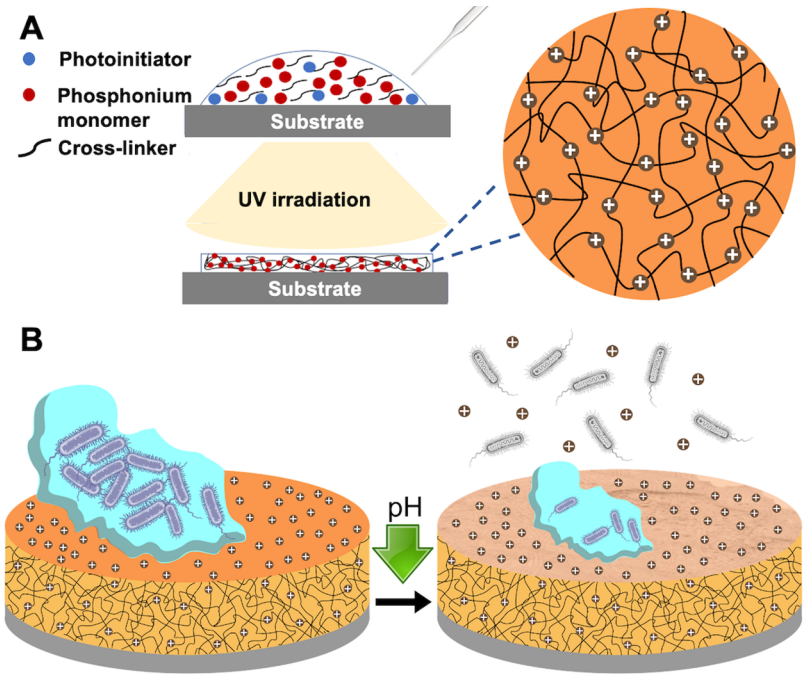

Figure 1. pH-sensitive phosphonium coatings. (A) Coating preparation by UV curing. (B) Phosphonium coatings were triggered to break down under mildly acidic conditions, releasing phosphonium species and bacteria.

on the antibacterial activity of Ag^+ that is released from silver nanoparticles, irradiation of a graphene oxide/silver nanoparticle/collagen composite coating with 660 nm light generated reactive oxygen species, leading to high antibacterial activity of the coating.[34] Near-infrared light irradiation (700−1100 nm) of two-dimensional Pb−Ag nanosheets led to the enhanced release of Ag^+, and when combined with plasmonic heating, it resulted in the synergistic killing of bacteria.[35] Induction heating induced by an alternating magnetic field was recently used to increase the rate of rifampicin (antibiotic) release from a poly(ester amide) coating that had a glass-transition temperature just above the physiological temperature, with the mild heating also acting as an enhancement to the antibiotic for killing bacteria and preventing biofilm formation.[36] Self-defensive coatings that release antibiotics in response to bacteria have also been reported.[37,38] Multilayer films, composed of chitosan and hyaluronic acid (HA) conjugated to the antimicrobial peptide cateslytin, were cleaved by hyaluronidase that was secreted by *Staphylococcus aureus* (*S. aureus*), thereby facilitating access to the peptide and enabling it to exert its antibacterial activity.[37] In another example, a multilayered coating composed of HA and poly(L-lysine) underwent degradation in response to hyaluronidase and chymotrypsin secreted by the bacteria, resulting in the continual shedding of the outer layer of the coating, effectively removing the adhered bacteria.[38]

Among the stimuli that are intrinsically associated with biofilms, the local reduction in pH[33,39] resulting from the production of organic acids[40] can be exploited for the development of stimuli-responsive surfaces, as pH change can alter the solubility of amine or carboxylic acid-containing polymers or cleave chemical linkages including imines, amides, esters, or acetals.[29,32] Bilayered films composed of chitosan and poly(acrylic acid) loaded with tobramycin were developed.[41] At pH 4.0, the poly(acrylic acid) (PAA) layer collapsed, allowing the chitosan layer to swell and release tobramycin. Multilayered coatings composed of montmorillonite clay nanoplatelets and PAA loaded with cationic gentamycin were also prepared and exhibited pH-dependent gentamycin release due to the disruption of ionic bonding upon acidification.[42] Acid-responsive imine linkages were also used to immobilize vancomycin in nonfouling PEG-based hydrogels[43] or cationic amine-coated silver nanoparticles in hydrogels based on oxidized polysaccharides.[44] In addition, a pH-responsive antibacterial coating was prepared from 4-(vinyloxy)butyl methacrylate polymers conjugated to 6-chloropurine via a hemiaminal ether linkage.[45] Systems exploiting combinations of multiple stimuli have also been reported.[46−48]

Despite the progress described above, to the best of our knowledge, stimuli-responsive phosphonium antibacterial surfaces have not yet been developed. Phosphonium surfaces can present different properties than their ammonium analogues due to their different charge distributions and can provide advantages such as enhanced thermal stability.[49] While in the past we have developed antibacterial phosphonium surfaces using chemically stable cross-linkers or semi-interpenetrating networks,[24,25] we now present the development of phosphonium surfaces incorporating pH-sensitive acetal cross-linkers (Figure 1). The incorporation of different phosphonium monomers and their influence on the physicochemical and antibacterial properties of the coatings was explored. Using *Escherichia coli* (*E. coli*) and *S. aureus* as representative Gram-negative and Gram-positive bacteria, respectively, we demonstrated that the antibacterial properties of the surfaces depend on the phosphonium structure, pH, and the bacterial strain.

EXPERIMENTAL SECTION

General Materials and Methods. Tributyl(4-vinylbenzyl)-phosphonium chloride (BuP), triethyl(4-vinylbenzyl)phosphonium chloride (EtP), triphenyl(4-vinylbenzyl)phosphonium chloride (PhP), and tris(hydroxypropyl)(4-vinylbenzyl)phosphonium chloride (HyP) were prepared as previously reported (Figures S1−S4).[25,50,51] Acetal (XA) and ketal (XK) cross-linkers were also synthesized

https://doi.org/10.1021/acsapm.4c00197
ACS Appl. Polym. Mater. 2024, 6, 6208−6218

according to a previous report (Figures S5 and S6).[52] Hydrogen peroxide (30% in water), sulfuric acid (90−98%), and the Live/Dead BacLight Bacterial Viability Kit (L7007) were purchased from Thermo Fisher Scientific (Mississauga, Canada). Ammonia (7 M in methanol) was purchased from Alfa Aesar (Massachusetts). Sodium acetate, acetic acid, sodium phosphate dibasic, sodium phosphate monobasic, methanol, and toluene (glass-distilled) were purchased from Caledon (Halton Hills, Ontario, Canada). Sodium chloride was purchased from Ambeed (Illinois). Anhydrous ethanol was purchased from Greenfield global (Brampton, Ontario, Canada). Potassium chloride and potassium phosphate monobasic were purchased from EMD Millipore (India). Triethylamine (glass-distilled), 3-(trimethoxysilyl)propyl methacrylate, 2-hydroxy-2-methylpropiophenone (HMP), fluorescein sodium salt, cetyltrimethylammonium chloride solution (25 wt % in water), hydrochloric acid (37%), tryptic soy broth (TSB), Mueller−Hinton broth, agar powder, chloramphenicol, and ampicillin were purchased from Millipore Sigma (Oakville, Canada). Ti (Ti6Al4V) foil (Gr 5, ASTM F136, 0.05 mm thickness) was purchased from Shaanxi Yunzhong Metal Technology Co., Ltd. (Shaanxi, China). Ultraviolet−visible (UV−vis) spectroscopy was performed using a Varian Cary 300 spectrometer at room temperature.

Substrate Preparation. Ti foil was cut into squares (1 cm × 1 cm) and then treated with piranha solution (3:1 (v/v) H_2SO_4:H_2O_2) for 2 min. Substrates were incubated for 30 min in 5:1:1 H_2O:H_2O_2:NH_3 in MeOH and then for 30 min in 3:1:1 H_2O:H_2O_2:HCl.[53] The foil was then rinsed thoroughly with deionized water (3 × 10 mL), followed by acetone, dried under nitrogen, and used immediately.

Glass slides were cut into squares (1 cm × 1 cm) and activated only with the piranha solution.[54] The treated substrates were then immersed in a 2% (v/v) solution of 3-(trimethoxysilyl)propyl methacrylate in 50 mL of anhydrous toluene overnight at room temperature under nitrogen. After silanization, the substrates were sonicated consecutively in toluene, toluene:MeOH (1:1), and MeOH for 5 min each, dried under vacuum, and used immediately.

Coating Preparation. The coating formulation consisted of 5% HMP, 45% phosphonium monomer (BuP, EtP, PhP, or HyP), and 50% acetal cross-linker (XA or XK) diluted with methanol (~15 μL per 30 mg of formulation). The formulation was cast on either Ti foil or glass slides (treated as above) using a 50.8 μm Meyer rod (20 mm rod diameter). To prepare free-standing films for cure percentage determination, the glass slide ends were wrapped with tape to create a spacer, and then after casting the film, another slide was placed on top of the substrate. Photopolymerization was performed by passing the samples five times through a UV conveyor system (UV Process and Supply Inc., Illinois), equipped with a mercury lamp with an energy and power density of UVA (1784 mJ cm^{-2}, 192 mW cm^{-2}), UVB (1647 mJ/cm^2, 178 mW cm^{-2}), UVC (369 mJ cm^{-2}, 43 mW cm^{-2}), and UVV (1869 mJ cm^{-2}, 199 mW cm^{-2}) at a speed of ~0.06 m/s. The thickness of the coating (50 ± 4.5 μm) was confirmed using an IP65 digital caliper. The freshly prepared coatings were washed with deionized water to remove the unreacted material until no further traces of formulation components were detected by ultraviolet−visible (UV−vis) spectroscopy (260 nm corresponding to the phenyl moiety of the phosphonium monomers).

Coating Properties. *Cure Percentage Determination.* Immediately after curing, the free-standing films were dried to measure their initial mass (m_i) and then immersed in deionized water to remove unreacted or soluble oligomeric components. The water was repeatedly changed until no leachable components were detected by UV−vis spectroscopy (260 nm). The films were then dried in vacuo at 37 °C over 24 h and then weighed again (m_f). The cure percentage was calculated using eq 1

$$\text{cure percentage} = \frac{m_f}{m_i} \times 100 \tag{1}$$

Charge Density Determination. The coating's surface charge density (c^+) was calculated based on adsorption of the anionic fluorescein dye.[55] After preparation and washing, the coated substrates (glass) were immersed in an aqueous 1% w/v fluorescein sodium salt solution (10 mL) for 30 min. After rinsing extensively with deionized water (3 × 10 mL), the coating was placed in 0.1% (v/v) aqueous cetyltrimethylammonium chloride (10 mL) and shaken for 20 min. Phosphate buffer (pH 8; 10 mM; 10 mL) was added, the absorbance of the released dye was measured at 501 nm (A_{501}), and the concentration of fluorescein ($c_{\text{fluorescein}}$) was determined based on the extinction coefficient (ε) of fluorescein at 501 nm (77,000 cm^{-1} M^{-1}).[50] Charge density was calculated based on $c_{\text{fluorescein}}$, assuming that each molecule of fluorescein was bound to one accessible cation (eq 2), where N is Avogadro's number (6.022 × 10^{23}), A is the coating surface area (1 cm^2), and V is the volume in which the fluorescein concentration was measured.

$$c^+ = \frac{c_{\text{fluorescein}} \times V \times N}{A} \tag{2}$$

Water Contact Angle (WCA). The coatings (glass substrate) were washed and dried prior to analysis. Measurements were performed by the sessile drop method (10 μL of distilled water) using a goniometer (Kruss DSA100 Drop Shape Analyzer) equipped with a camera. Values were obtained after 1 min of droplet incubation on the surface. Angle analysis was performed by Drop Shape Analysis software using the Laplace−Young fitting. A minimum of five WCAs were obtained for each of the three separate coatings, and the results are reported as the mean ± standard deviation.

pH-Dependent Degradation. Phosphonium coatings (1 cm × 1 cm, glass substrate, 50 μm thickness) were each placed in a glass vial and immersed in 1.5 mL of acetate buffer (10 mM, pH 4.5, 5.0, or 5.5) or phosphate buffer (10 mM pH 6.5 or 7.4) and then incubated at 37 °C. Aliquots were taken at different time points, and their UV−vis absorbances were measured at 260 nm (BuP coatings) or 275 nm (PhP coatings). The aliquots were returned to the glass vial for further incubation if the absorbance was below 0.1. If the absorbance was greater than 0.1, the media was discarded and replaced with a fresh buffer. At the end of the experiment, five drops of 6 M HCl were added to adjust the pH to 3. After 16 h, by which time complete coating degradation was achieved, the absorbance was measured and used to determine the absorbance at 100% degradation, allowing calculation of the cumulative percent phosphonium release at the evaluated time points. The experiments were performed in triplicate for each coating and pH, and the results are provided as the mean ± standard deviation.

Bacterial Culture. *S. aureus* (ATCC 6538) and *E. coli* (ATCC 29425) were purchased from the American Type Culture Collection. *S. aureus* (ATCC 6538) and *E. coli* (DH5α) expressing the green fluorescence protein (GFP) (*S. aureus*-GFP and *E. coli*-GFP) were prepared by transformation using electroporation with the plasmid pCG44.[56,57] The plasmids were maintained by culturing *S. aureus* in chloramphenicol at 10 μg mL^{-1} and *E. coli* in 100 μg mL^{-1} ampicillin. All bacterial glycerol stocks (1:1 in 50% glycerol) were stored at −80 °C. For an overnight bacterial culture, a sterile loop was used to scrape a sample of the frozen stock and the sample was added into 5 mL of TSB and incubated at 37 °C for 16 h under static conditions. The overnight culture was then diluted to 10^6 or 10^7 CFU mL^{-1} according to the optical density at λ = 600 nm (OD_{600}) (*E. coli* OD_{600} ≈ 0.2 at 10^7 CFU mL^{-1}, *S. aureus* OD_{600} ≈ 0.3 at 10^8 CFU mL^{-1}) for subsequent antimicrobial assays.

For agar plating, tryptic soy agar (TSA) was prepared by mixing 15 g of agar powder per 1 L of TSB.

Effect of Coating Degradation Products on Bacteria. Coated Ti foils (1 cm^2, 50 ± 4.5 μm thickness) were incubated in 1.5 mL of either pH 5.0 (10 mM acetate buffer) or pH 7.4 (10 mM phosphate buffer) at 37 °C for 7 days. A control consisted of a pH 7.4 buffer incubated with an uncoated Ti foil. The pH 5.0 solution was then adjusted to pH 7.4 with NaOH, and the coating solutions were sterilized by filtration through a 0.2 μm filter. 50 μL of the coating solution was then combined with 50 μL of the bacterial suspension (10^6 CFU mL^{-1} in Mueller−Hinton broth), and the resulting suspension was added into a 96-well plate. The plate was incubated at 37 °C for 16 h, and then, bacterial viability was determined by a drop

https://doi.org/10.1021/acsapm.4c00197
ACS Appl. Polym. Mater. 2024, 6, 6208−6218

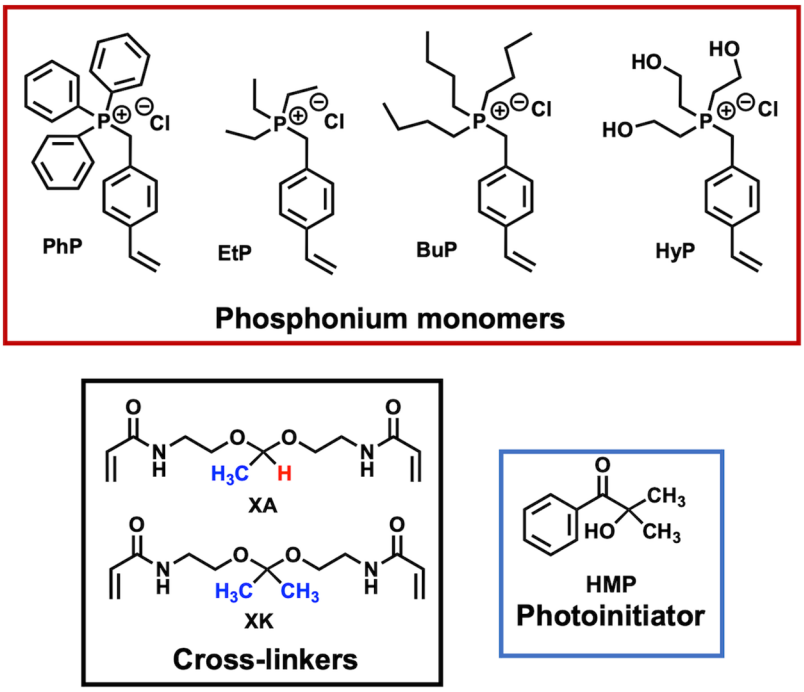

Figure 2. Chemical structures of the selected monomers, cross-linkers, and the photoinitiator.

plate method. The bacterial suspensions in each well were serially diluted (10-fold) in sterile PBS and plated (10 μL) onto a TSA plate. TSA plates were left to air-dry for 30 min before incubation at 37 °C for 16 h. CFUs were counted to determine the survival percentage versus the control with an untreated suspension of bacteria. Each coating was evaluated in triplicate, and the results are provided as the mean ± standard deviation.

Imaging and Quantification of GFP-Expressing Bacteria on the Coatings. After an overnight culture as described above, the bacterial suspension was centrifuged at 1000 rpm (168 relative centrifugal force), the supernatant was discarded, and the resulting bacteria were resuspended in sterile water twice and then centrifuged again. For *S. aureus*-GFP, the final pellet was resuspended in either acetate buffer (10 mM, pH 5.0) or phosphate buffer (10 mM, pH 7.4) at 10^7 CFU mL^{-1}. For *E. coli*, the pellet was resuspended at 10^7 CFU mL^{-1} in a Mueller−Hinton broth adjusted to either pH 5.0 or pH 7.4 using 0.5 M HCl or 0.5 M NaOH in water. Coated (45 μm thickness) and uncoated control Ti foils were sterilized by immersion in 70% ethanol for 30 min and then air-dried before use. The substrates were each placed in a well of a 6-well plate and then immersed in 4 mL of the bacterial suspension. The samples were incubated at 37 °C for 16 h and then gently rinsed with distilled water before imaging using a Nikon Eclipse Ti2E inverted deconvolution microscope (Nikon Instruments Canada Inc., Mississauga, Canada) at 20× magnification using 465−485 nm excitation and 499−530 nm emission filters. Imaris software (version 8.0.3, Bitplane, Belfast, U.K.) was used for image analysis to count the bacteria adhered to the surface at five random areas per coating (162 μm × 162 μm). Each coating was evaluated in triplicate, and the results are provided as the mean ± standard deviation. The data were analyzed using an ANOVA, followed by a Tukey post hoc test.

Live/Dead Imaging of Bacteria on the Coatings. *E. coli* and *S. aureus* bacterial suspensions were prepared and incubated with coated or uncoated control Ti foils as described in the preceding section, except that bacterial strains not expressing GFP were used. After 16 h of incubation, the coatings were removed from the bacterial suspension, rinsed with deionized water, and then stained using a Live/Dead BacLight Bacterial Viability Kit containing SYTO9 to detect viable cells and propidium iodide (PI) to detect dead cells. The stain was prepared according to the manufacturer's instructions, added directly onto the surfaces of all samples, and then incubated at room temperature for 10 min in the dark. The previously uncoated Ti foils incubated in bacteria were selected as the live control. For the dead control, these uncoated Ti foils were subjected to a heating shock treatment at 150 °C for 15 min. Imaging was performed using a Nikon Eclipse Ti2E microscope at 20× magnification. For excitation, a 465−485 nm filter was used, while for emission, filters of 499−530 nm (SYTO9) and 580−610 nm (propidium) were used. For quantitative analysis of the Live/Dead imaging, the Image-Pro v11 (Media Cybernetics, Rockville MD) cell biology protocol "live−dead" was used to calculate the % viable bacteria. The data were analyzed using an ANOVA, followed by a Tukey post hoc test.

Mammalian Cytotoxicity Assay. Solutions of coating degradation products (Figure S7) were prepared by incubating each coating in 1 M HCl for 48 h to achieve complete degradation of the networks. The pH of each solution was then adjusted to 7.4 using 1 M NaOH. A 3-(4,5-dimethylthiazol-2-yl)-2,5-diphenyltetrazolium bromide (MTT) assay on C2C12 mouse myoblast cells was then performed as previously reported.[58] The solution of coating degradation products was diluted 10-fold with the culture media and then passed through a 0.2 μm filter for sterilization to achieve a concentration of 225 μg mL^{-1} (based on the known quantity of polymer in the initial coating), which was then subjected to serial 2-fold dilutions to 3.5 μg mL^{-1}. Six replicates of each concentration were evaluated, and the results are presented as the mean ± standard deviation.

RESULTS AND DISCUSSION

Phosphonium Coating Preparation. The phosphonium monomers PhP, EtP, BuP, and HyP (Figure 2) were prepared as previously reported.[25,51] These monomers were selected for their cationic phosphonium centers, ease of synthesis of the styrenic derivatives, and potential for antibacterial activity resulting from their balance of hydrophobic and hydrophilic properties.[24,25,51,59−61] The selected cross-linkers were a bis(acrylamide) ketal based on acetone (XK) and a bis(acrylamide) acetal based on acetaldehyde (XA).[52] These linkers were previously shown to be cleaved under mildly acidic conditions, but at varying rates, with the ketal cleaved much more rapidly than the acetal.[52] HMP was selected as the photoinitiator for UV curing of the coatings.

https://doi.org/10.1021/acsapm.4c00197
ACS Appl. Polym. Mater. 2024, 6, 6208−6218

Fixing HMP at 5% (w/w), different coating formulations were initially prepared at varying cross-linker/monomer ratios ranging from 40:55 to 70:25 (w/w) (Table 1). To examine their potential to form cross-linked coatings, the formulations were cast onto glass substrates using a Meyer rod and cured by irradiation with UV light. The extent of cross-linking was assessed based on the cure percentage. At less than 50% cross-linker, successful coating preparation was not achieved, as the materials swelled and fragmented, making the measurement of cure percentage impossible, with the exception of the BuP system (23 ± 1%). At 50% cross-linker and above, the cure percentage exceeded 80% for the PhP and BuP networks. The EtP and HyP systems swelled considerably and rapidly delaminated from the surface, so they were not investigated further. To maximize the content of the active phosphonium monomer, formulations containing 5% HMP, 45% phosphonium monomer, and 50% cross-linker were selected for all subsequent studies with PhP and BuP. In addition to glass substrates, coatings were cast and cured on Ti foil, as Ti materials are commonly employed in orthopedic implants such as in joint prostheses, as well as screws and plates used in surgeries. These metallic implants are frequently associated with infections involving bacterial biofilms.[62,63] To achieve sufficient adhesion to Ti, the surface was first treated with 3-(trimethoxysilyl)propyl acrylate to establish a bonding between the cured formulation and the metal.[53]

Table 1. Effect of XK or XA Cross-Linker Percentage on the Cure Percentage for PhP and BuP Coatings Cast and Cured with UV Light on Glass Surfaces[a]

	XK wt %			XA wt %		
cure percentage	40	50	70	40	50	70
PhP	*F*	83 ± 2	87 ± 1	*F*	90 ± 2	91 ± 3
BuP	23 ± 1	94 ± 2	97 ± 3	*F*	82 ± 0.1	97 ± 2

[a]5 wt % HMP photoinitiator was used in each formulation, along with PhP or BuP to bring the composition to 100%. *F*, coating fragmented, making determination of the cure percentage impossible.

Phosphonium Coating Properties. The accessible surface charges were quantified for each phosphonium coating, as this property plays an important role in antibacterial activity, with a charge density of at least 10^{14} cations cm^{-2} generally required for bacterial killing.[64] Based on the fluorescein adsorption assay, there were at least 10^{16} cations cm^{-2} for both XA and XK coatings (Table 2). These values are within 1 order of magnitude of those reported for other recently reported charged, contact-active antibacterial surfaces.[65,66] The wettabilities of the phosphonium coatings were assessed using WCA measurements. All surfaces were hydrophilic (WCA range: 50−62°), presumably due to the amides and charged phosphonium groups on the coatings, with the BuP surfaces being a bit more hydrophobic than the PhP surfaces.

pH-Dependent Coating Degradation. The pH-dependent degradation of the BuP and PhP coatings was studied at 37 °C from pH 4.5 to 7.4, with pH 7.4 being the neutral physiological pH and pH 4.5 being the pH that can be obtained locally from a bacterial infection due to metabolic byproducts such as lactic acid produced by *S. aureus*[40] or acetic acid produced by *E. coli*.[67] Acetate buffer was used in the range of pH 4.5−5.5, while phosphate buffer was used in the range of pH 6.5−7.4. Although changing the buffer salts could potentially influence the hydrolysis rate, it was deemed necessary to ensure that each buffer system was used only in its appropriate buffering pH range. The degradation was assessed based on the release of species (e.g., triphenylphosphonium, or aldehyde/ketone from cross-linker cleavage) into solution, as measured by UV−vis spectroscopy. Coatings prepared from both BuP and PhP, along with the acetal cross-linker XA, were stable, with less than 10% of the degradation over 22 days (Figure 3A,B). These results are in agreement with a previous report where similar acetal-based cross-linkers exhibited minimal hydrolysis at pH 7.4 for 7 days.[52] On the other hand, both the BuP and PhP coatings prepared using the ketal cross-linker XK underwent substantial degradation over 14 days (Figure 3C,D). This result was expected as aliphatic ketals generally hydrolyze more rapidly than aliphatic acetals due to stabilization of the carbocationic transition state during hydrolysis by two pendent alkyl groups compared to one.[68] We also observed pH-dependent degradation rates for coatings containing the XK cross-linker, with degradation being complete at pH 4.5 in less than 2 days, whereas at pH 5, complete degradation required about 1 week. These differences between pH 4.5 and pH 5.0 aligned well with the rate of ketal hydrolysis being first order with respect to the hydronium ion[52,69] and thus ∼3-fold faster with each 0.5 decrease in pH unit. At pH 5.5−7.4, the hydrolysis was much slower, with 20−40% degradation observed for the PhP-XK coatings and ∼70% degradation for the BuP-XK coatings. While WCA measurements suggested that the BuP coatings were actually more hydrophobic, it is possible that the PhP coatings hydrolyzed more slowly as it was more difficult for water to penetrate the PhP coatings due to their more rigid aromatic structures and $\pi-\pi$ stacking. An unexpected result was the minimal pH-dependence of the coating hydrolysis between pH 5.5 and 7.4, particularly for BuP-XK coatings. Unlike simple ketal hydrolysis in solution, it appears that other factors such as water penetration into the coatings may dominate the hydrolysis rate under these conditions. Nevertheless, the results of these degradation studies demonstrated that coatings of varying stabilities could be achieved using the XK and XA cross-linkers and that pH-dependent degradation occurred at mildly acidic pH.

Antibacterial Activity of the Coatings. Coatings on Ti surfaces were then evaluated for their ability to release antibacterial species into solution in a pH-dependent manner. While styrenic phosphonium monomers and polymers have

Table 2. Charge Density (c^+) and Water Contact Angle (WCA) for Coatings with 45% Phosphonium Monomer, 5% HMP, and 50% Cross-Linker (w/w)

	XA		XK	
coating formulation	WCA (°)	c^+ (cations cm^{-2})	WCA (°)	c^+ (cations cm^{-2})
PhP	51 ± 2	$(2.2 \pm 1.2) \times 10^{16}$	55 ± 2	$(5.6 \pm 4.4) \times 10^{16}$
BuP	59 ± 0.2	$(1.8 \pm 6.4) \times 10^{16}$	62 ± 2	$(5.9 \pm 1.8) \times 10^{16}$

https://doi.org/10.1021/acsapm.4c00197
ACS Appl. Polym. Mater. 2024, 6, 6208−6218

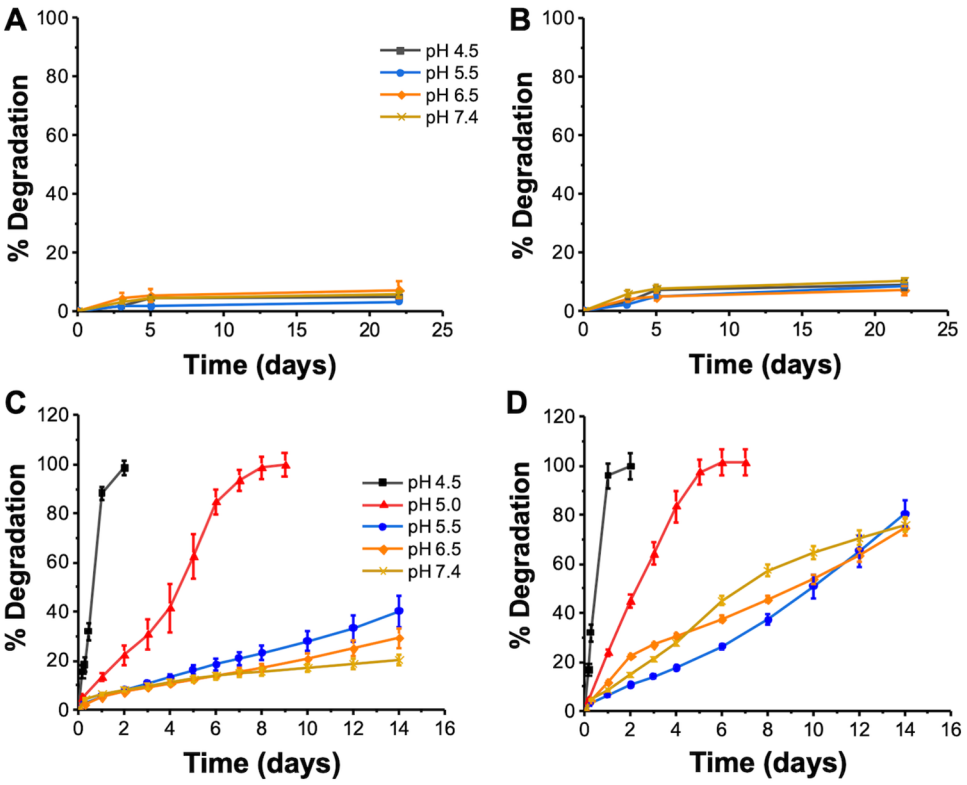

Figure 3. pH-dependent degradation of (A) PhP-XA, (B) BuP-XA, (C) PhP-XK, and (D) BuP-XK coatings at pH values from 4.5 to 7.4 (37 °C) assessed based on the release of degradation products into solution as measured by UV−vis spectroscopy.

been evaluated for their antibacterial activities in the past,[25,51,59,70] coatings reported here would release polymeric or oligomeric species that also contain hydroxyethylacrylamide moieties from the cross-linker (Figure S7). After washing the cured coatings thoroughly to remove any residual uncured monomer, cross-linker, or photoinitiator, they were incubated at either pH 5.0 or 7.4 for 7 days. The pH 5.0 solution was then adjusted to 7.4, and the pH 7.4 solutions of coating degradation products were added to suspensions of *E. coli* ATCC 29425 and *S. aureus* ATCC 6538 (10^6 CFU mL^{-1}) in Mueller−Hinton broth. After incubation for 16 h, the resulting suspensions were plated on agar to examine bacterial viability compared to bacterial suspensions exposed to control solutions at pH 5 or pH 7.4 that were incubated with uncoated Ti surfaces.

The extent of bacterial killing depended on the coating formulation and pH. All coatings containing the XA cross-linker led to minimal killing of bacteria, regardless of pH (Figure 4). Kanazawa et al. previously found that the inhibitory concentrations for polymers prepared from BuP and PhP were ∼10 $\mu g\ mL^{-1}$ against *S. aureus* and >100 $\mu g\ mL^{-1}$ against *E. coli*, while monomeric analogues had even higher minimal inhibitory concentrations.[59] Given their low extent of degradation and release of bioactive phosphonium species during the one-week incubation period, the concentration of released phosphonium species from the XA coatings was not sufficiently high to fully inhibit bacterial growth. Nevertheless, for *S. aureus*, 10−20% killing for BuP-XA and 20−30% killing for PhP-XA were observed, indicating that *S. aureus* was more susceptible than *E. coli* to the low concentration of phosphonium species released from the coatings and also that the released PhP species were somewhat more active than the corresponding BuP species. The differences in suscepti-

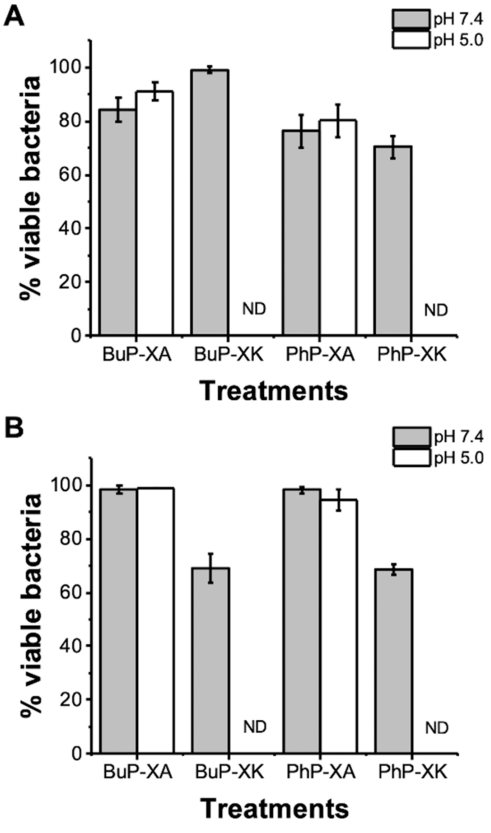

Figure 4. % Viable bacteria of (A) *S. aureus* and (B) *E. coli* incubated with a degraded coating solution at pH 5.0 and pH 7.4 determined by the drop plate method. Error bars correspond to the standard deviation (N = 3 surfaces).

https://doi.org/10.1021/acsapm.4c00197
ACS Appl. Polym. Mater. 2024, 6, 6208−6218

bility between *S. aureus* (Gram-positive) and *E. coli* (Gram-negative) may have arisen from their different membrane structures. Gram-negative bacteria have an additional outer membrane and tend to be more effectively killed through hydrophobic insertion mechanisms, whereas Gram-positive bacteria lack this outer membrane and favor charge-based killing mechanisms.[71] The higher activity of the slightly less hydrophobic PhP species compared to the BuP species is also in agreement with the results previously reported by Kanazawa et al.[59] At pH 7.4, ∼30% killing was generally observed for the XK coatings, which can be attributed to some hydrolysis of the ketal cross-linker and release of phosphonium (20−30%) from these coatings over 1 week. Notably, at pH 5.0, for both the BuP-XK and PhP-XK coatings, no viable CFUs were detected, indicating that the coating degradation products were able to successfully kill both *E. coli* and *S. aureus*, corresponding to at least a 3-log kill based on the assay.

The effects of the coatings on bacteria seeded directly on the coatings were also examined. The coated Ti surfaces were incubated with *S. aureus*-GFP or *E. coli*-GFP at pH 5.0 or 7.4 for 16 h. After carefully rinsing the surfaces to remove nonadhered bacteria, they were imaged by fluorescence microscopy and the density of bacteria was quantified and compared to control Ti surfaces at each pH (Figures 5 and S8 and S9). In the case of *S. aureus*, the BuP-XA coatings led to a modest ∼10% reduction in the densities of bacteria compared to the control, while the PhP-XA surface led to ∼30% reduction. There were no statistically significant differences observed between pH 7.4 and 5.0 for these coatings with *S. aureus*. On the other hand, both BuP-XK and PhP-XK coatings exhibited large differences in activity between pH 7.4 and 5.0 with the coatings behaving similarly to the control surface at pH 7.4, but with reductions in *S. aureus* of ∼90 and ∼95%, respectively, at pH 5.0. These trends are in line with the higher antibacterial activity of the released PhP species compared to the BuP species toward *S. aureus* as described above (Figure 4). Overall, these results indicate the importance of coating degradation and substantial phosphonium release for effectively inhibiting the growth of *S. aureus* on the coating surfaces in this assay.

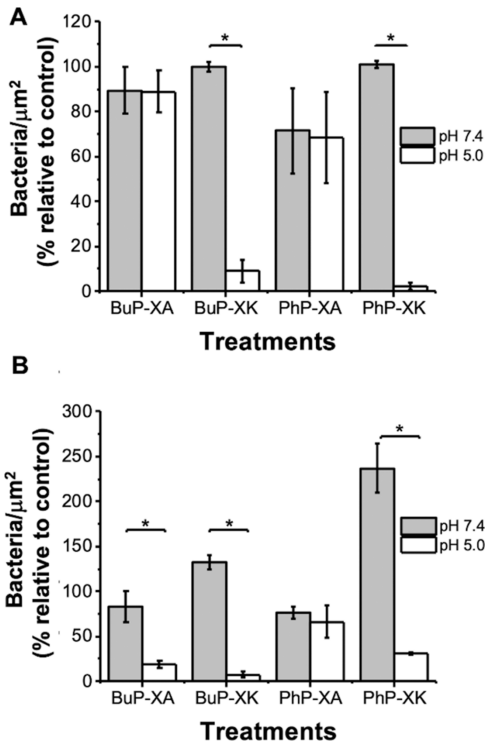

Figure 5. Relative numbers of bacteria count adhered to the surface: (A) *S. aureus*-GFP and (B) *E. coli*-GFP on coated Ti surfaces incubated at either pH 7.4 or pH 5.0 (normalized to an uncoated surface defined as 100% at each pH). Error bars correspond to the standard deviations (N = 3 surfaces, 5 areas per surface measured). * indicates treatment pairs that were significantly different statistically ($p < 0.05$).

The densities of *E. coli* on the coatings varied greatly, depending on the formulation and the pH. For example, at pH 7.4, both BuP-XK and PhP-XK coatings had higher *E. coli* densities than the control Ti foil, indicating the preference of *E. coli* for the polymer-coated surfaces. This result might be attributed to *E. coli*'s[72,73] lower tendency to form biofilms compared to *S. aureus* ATCC 6538, and thus, there is a strong influence of the underlying surface. However, at pH 5.0, the density of bacteria was suppressed by 95 and 70% compared to the control for BuP-XK and PhP-XK, respectively, indicating that the degradation of these coatings was able to suppress *E. coli* colonization. BuP-XA at pH 7.4 and PhP-XA at pH 5.0 resulted in intermediate densities of bacteria, ranging from 20 to 70% of the control, presumably due to the presence of phosphonium groups suppressing to some extent *E. coli* colonization. Even with its slow degradation rate, the BuP-XA coating was able to suppress the *E. coli* density by ∼80%, likely because of there being some activity of the tributyl(4-vinylbenzyl)phosphonium moiety immobilized on the surface and further enhanced by a small amount of phosphonium release at pH 5.0. Overall, there was a trend toward higher antibacterial activity for the BuP coatings compared to the PhP coatings against *E. coli* colonization of the surface. The BuP coatings may be more effective against *E. coli* due to their higher hydrophobicity, which is important for the membrane disruption mechanism involved in the killing of Gram-negative bacteria.[20,74] It should also be noted that the susceptibility of the bacteria to the substrate and released biocidal molecules might also vary with pH as we observed a trend toward higher activity at pH 5 compared to 7.4, and Kanazawa et al. also previously reported a low activity for polymers prepared from BuP and PhP as well as their monomeric analogues against *E. coli* at neutral pH.[59]

Live/dead staining was performed for the more active surfaces containing the XK ketal cross-linker, and the effects of pH were probed. In this assay, the live bacteria appear green as a result of the SYTO9 stain, whereas the dead bacteria appear red from the propidium iodide. The images revealed that both BuP-XK and PhP-XK coatings had high fractions of live *S. aureus* (Figure 6A,B) and *E. coli* (Figure 6C,D) at pH 7.4. At pH 5.0, the percentage of live bacteria was significantly lower for both the BuP-XK and PhP-XK coatings and both strains of bacteria. However, bacteria were still present on the surfaces, even at pH 5. This observation can be attributed to the relatively low (∼10%) degradation of the coatings at the 16 h time point, when imaging was performed. Overall, the live/dead results were in general agreement with the quantification of live GFP-expressing bacteria described above (Figure 5).

The results of our antibacterial studies can be compared with those of previously reported pH-responsive antibacterial coatings. For example, multilayered coatings composed of chitosan and PAA loaded with tobramycin effectively

https://doi.org/10.1021/acsapm.4c00197
ACS Appl. Polym. Mater. 2024, 6, 6208−6218

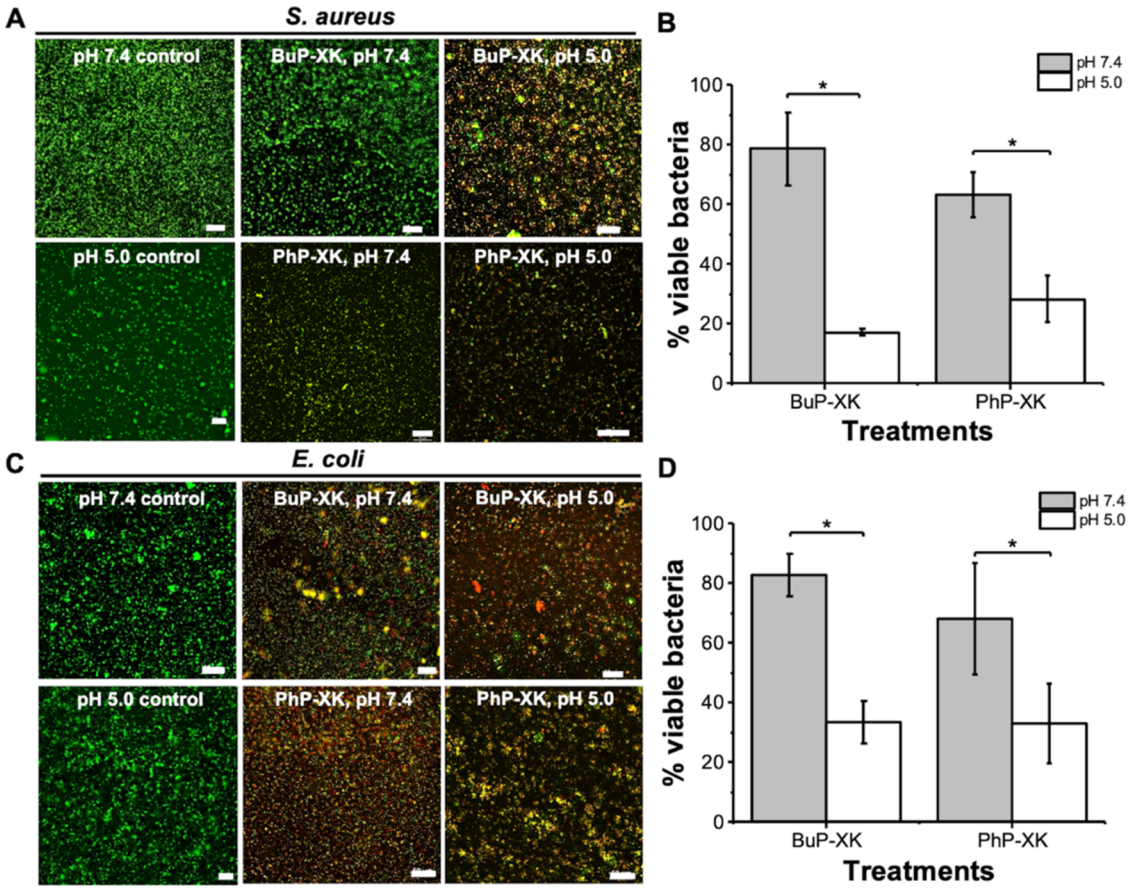

Figure 6. Live/dead staining of *S. aureus* and *E. coli* on a control Ti surface (uncoated) and XK cross-linker-containing coatings on Ti at pH 7.4 and 5.0: (A) fluorescence microscopy images of *S. aureus*; (B) % viable *S. aureus* calculated from the images; (C) fluorescence microscopy images of *E. coli*; and (D) % viable *E. coli* calculated from the images. Error bars correspond to the standard deviations (N = 3 surfaces, 5 images per surface). Scale bar is 50 μm. * indicates treatment pairs that were significantly different statistically ($p < 0.05$).

prevented colonization when incubated for 2 h with 10^4 CFU mL^{-1} *S. aureus* but were not effective with 10^5 CFU mL^{-1}.[41] Multilayered coatings composed of PAA, clay, and gentamycin were able to kill up to 10^8 CFU mL^{-2} with 9.5 bilayers, with a lower killing for coatings with fewer layers.[42] PEG-based hydrogels with imine-conjugated vancomycin killed 10^6 CFU mL^{-1} *S. aureus* over ~4 h when loaded with 250 μg mL^{-1} vancomycin.[43] Coatings prepared from 4-(vinyloxy)butyl methacrylate polymers with 6-chloropurine conjugated by hemiaminal ethers provided a >99.9% reduction when incubated with 10^4 CFU cm^{-2} *S. aureus* or *E. coli* for 24 h.[45] Thus, our pH-responsive phosphonium coatings appear to exhibit comparable antibacterial activity to these coatings while being very simple to prepare.

Cytotoxicity to Mammalian Cells. C2C12 mouse myoblast cells were used to assess the toxicity of the coating degradation products to mammalian cells. The degradation products were generated by incubating the coatings in 1 M HCl, and the solutions were adjusted to neutral pH and diluted in cell culture media. Most of the released polymers had IC_{50} values in the range of 50−100 μg mL^{-1}, with the IC_{50} of the PhP-XK products being a bit higher (Figure 7). These results are in general agreement with what we previously reported for phosphonium polymers with different substituents such as ethyl, butyl, phenyl, and 3-hydroxypropyl,[58] indicating that the incorporation of the cross-linker did not have a major effect. The mechanism of phosphonium cytotoxicity is thought to involve cell membrane disruption.[74] The BuP-XA coating degradation products had surprisingly low toxicity. Since the XA cross-linked coatings degrade more slowly, it is possible that these materials had not degraded fully to molecularly dissolved species and therefore exhibited lower toxicity. However, this will require further investigation. Overall, while phosphonium cytotoxicity is not a major concern for applications such as surface decontamination outside the body,

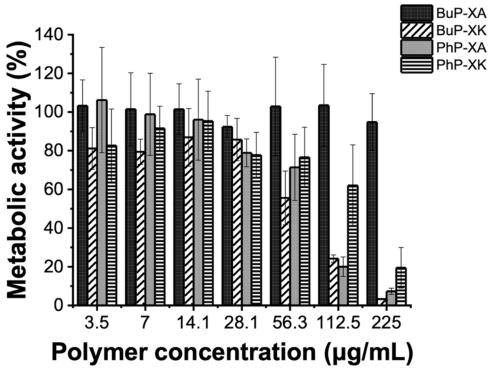

Figure 7. Metabolic activity of C2C12 cells (compared to control cells exposed to only culture media) after exposure to varying concentrations of phosphonium degradation products of the coatings, as measured by an MTT assay. Error bars correspond to the standard deviation on six replicates.

https://doi.org/10.1021/acsapm.4c00197
ACS Appl. Polym. Mater. 2024, 6, 6208−6218

for potential applications in vivo, phosphonium toxicity to mammalian cells must be balanced with their antibacterial activity.

CONCLUSIONS

Phosphonium cation-containing coatings were prepared using a combination of four different phosphonium monomers and acetal (XA) or ketal (XK) cross-linkers. Both the BuP and PhP monomers provided coating materials with a high cure percentage and at least 10^{16} accessible cations cm^{-2} when combined with 50% (w/w) of XA or XK. Coating degradation studies revealed that XA coatings were very stable from pH 7.4 to 4.5, with less than 10% degradation over 3 weeks, whereas the XK coatings degraded completely over a few days at pH 4.5, over a week at pH 5.0, and more slowly at pH 5.5−7.4. The rapid degradation of the XK coatings led to the release of antibacterial phosphonium species, which were capable of effectively killing both *S. aureus* and *E. coli* in suspension, as demonstrated using the drop plate method. Fluorescence microscopy imaging of coated Ti surfaces incubated with GFP-expressing *S. aureus* and *E. coli* showed that while bacteria grew on XA surfaces at moderate levels regardless of pH, and on XK surfaces at pH 7.4, XK coatings led to >90% suppression of bacterial growth on the surfaces at pH 5.0. These results were supported by live/dead imaging of bacteria on the surfaces. This study indicates that the use of pH-sensitive cross-linkers can be an effective approach for suppressing the colonization of bacteria on surfaces in a pH-dependent manner. Further work will be directed toward completely suppressing bacterial growth on the coatings through the incorporation of multiple inhibitory mechanisms and toward eliminating the adhesion of dead bacteria to the surface, thereby inhibiting biofilm development over the longer term.

ASSOCIATED CONTENT

Supporting Information

The Supporting Information is available free of charge at https://pubs.acs.org/doi/10.1021/acsapm.4c00197.

NMR spectra of the monomers and cross-linkers, structures of coating degradation products, fluorescence microscopy images of GFP-expressing bacteria on surfaces (PDF)

AUTHOR INFORMATION

Corresponding Author

Elizabeth R. Gillies − *School of Biomedical Engineering, The University of Western Ontario, London, Ontario N6A 5B9, Canada; Department of Chemistry, The University of Western Ontario, London, Ontario N6A 5B7, Canada; Department of Chemical and Biochemical Engineering, The University of Western Ontario, London, Ontario N6A 5B9, Canada;* orcid.org/0000-0002-3983-2248; Email: egillie@uwo.ca

Authors

Mónica Vásquez Peña − *School of Biomedical Engineering, The University of Western Ontario, London, Ontario N6A 5B9, Canada*

Karen Nygard − *The Biotron Experimental Climate Change Research Centre, The University of Western Ontario, London, Ontario N6A 5B7, Canada*

Paul J. Ragogna − *Department of Chemistry, The University of Western Ontario, London, Ontario N6A 5B7, Canada; Surface Science Western, London, Ontario N6G 0J3, Canada;* orcid.org/0000-0003-2727-7635

Complete contact information is available at: https://pubs.acs.org/10.1021/acsapm.4c00197

Notes

The authors declare no competing financial interest.

ACKNOWLEDGMENTS

The authors thank the Western Bone and Joint Institute (Catalyst Grant), the Natural Sciences and Engineering Research Council of Canada Discovery Grants Program (RGPIN-2021-03950 to ERG; RGPIN-2021-04377 to PJR), and the Canada Research Chair program (CRC-2020-00101 to ERG) for funding and CONACYT (Mexico) for MVP's fellowship. The authors acknowledge the Heinrichs laboratory for providing the GFP-expressing bacteria, Syensqo for supplying organophosphine starting materials, and the Biotron Integrated Microscopy Facility for assistance with fluorescence microscopy.

REFERENCES

(1) DeFlorio, W.; Liu, S.; White, A. R.; Taylor, T. M.; Cisneros-Zevallos, L.; Min, Y.; Scholar, E. M. Recent Developments in Antimicrobial and Antifouling Coatings to Reduce or Prevent Contamination and Cross-Contamination of Food Contact Surfaces by Bacteria. *Compr. Rev. Food Sci. Food Saf.* **2021**, *20*, 3093−3134.

(2) Sadrizadeh, S.; Aganovic, A.; Bogdan, A.; Wang, C.; Afshari, A.; Hartmann, A.; Croitoru, C.; Khan, A.; Kriegel, M.; Lind, M. A Systematic Review of Operating Room Ventilation. *J. Building Eng.* **2021**, *40*, No. 102693, DOI: 10.1016/j.jobe.2021.102693.

(3) Qiu, H.; Si, Z.; Luo, Y.; Feng, P.; Wu, X.; Hou, W.; Zhu, Y.; Chan-Park, M. B.; Xu, L.; Huang, D. The Mechanisms and the Applications of Antibacterial Polymers in Surface Modification on Medical Devices. *Front. Bioeng. Biotechnol.* **2020**, *8*, 910 DOI: 10.3389/fbioe.2020.00910.

(4) Wang, J.; Liu, J.; Wang, X.; Aleem, A. R.; Song, Z.; Kipper, M. J.; Tang, J. Smart Sensing of Bacterial Contamination on Fluorescent Cotton Fabrics (FCF) by Nontoxic Eu^{3+}-Induced Polyelectrolyte Nano-Aggregates (EIPAS). *Dyes Pigm.* **2020**, *181*, No. 108536, DOI: 10.1016/j.dyepig.2020.108536.

(5) Abebe, G. M. The Role of Bacterial Biofilm in Antibiotic Resistance and Food Contamination. *Int. J. Microbiol.* **2020**, *2020*, No. 1705814, DOI: 10.1155/2020/1705814.

(6) Vigeant, M. A.-S.; Ford, R. M.; Wagner, M.; Tamm, L. K. Reversible and Irreversible Adhesion of Motile *Escherichia coli* Cells Analyzed by Total Internal Reflection Aqueous Fluorescence Microscopy. *Appl. Environ. Microbiol.* **2002**, *68*, 2794−2801.

(7) Schuster, J. J.; Markx, G. H.Biofilm Architecture. In *Productive Biofilms*; Springer, 2013; Vol. *146*, pp 77−96 DOI: 10.1007/10_2013_248.

(8) Michaelis, C.; Grohmann, E. Horizontal Gene Transfer of Antibiotic Resistance Genes in Biofilms. *Antibiotics* **2023**, *12*, 328.

(9) Ciofu, O.; Moser, C.; Jensen, PØ.; Høiby, N. Tolerance and Resistance of Microbial Biofilms. *Nat. Rev. Microbiol.* **2022**, *20*, 621−635.

(10) Li, W.; Thian, E. S.; Wang, M.; Wang, Z.; Ren, L. Surface Design for Antibacterial Materials: From Fundamentals to Advanced Strategies. *Adv. Sci.* **2021**, *8*, No. 2100368, DOI: 10.1002/advs.202100368.

(11) Zhao, C.; Zhou, L.; Chiao, M.; Yang, W. Antibacterial Hydrogel Coating: Strategies in Surface Chemistry. *Adv. Colloid Interface Sci.* **2020**, *285*, No. 102280.

(12) Pandey, L. M. Design of Biocompatible and Self-Antibacterial Titanium Surfaces for Biomedical Applications. *Curr. Opin. Biomed. Eng.* **2023**, *25*, No. 100423.
(13) Ahmed, W.; Zhai, Z.; Gao, C. Adaptive Antibacterial Biomaterial Surfaces and Their Applications. *Mater. Today Bio* **2019**, *2*, No. 100017.
(14) Yu, Q.; Zhang, Y.; Wang, H.; Brash, J.; Chen, H. Anti-Fouling Bioactive Surfaces. *Acta Biomater.* **2011**, *7*, 1550−1557.
(15) Chen, P.; Lang, J.; Zhou, Y.; Khlyustova, A.; Zhang, Z.; Ma, X.; Liu, S.; Cheng, Y.; Yang, R. An Imidazolium-Based Zwitterionic Polymer for Antiviral and Antibacterial Dual Functional Coatings. *Sci. Adv.* **2022**, *8*, No. eabl8812, DOI: 10.1126/sciadv.abl8812.
(16) Tang, S.; Zheng, J. Antibacterial Activity of Silver Nanoparticles: Structural Effects. *Adv. Healthcare Mater.* **2018**, *7*, No. 1701503, DOI: 10.1002/adhm.201701503.
(17) Hans, M.; Mathews, S.; Mücklich, F.; Solioz, M. Physicochemical Properties of Copper Important for Its Antibacterial Activity and Development of a Unified Model. *Biointerphases* **2016**, *11*, No. 018902, DOI: 10.1116/1.4935853.
(18) Chug, M. K.; Brisbois, E. J. Recent Developments in Multifunctional Antimicrobial Surfaces and Applications toward Advanced Nitric Oxide-Based Biomaterials. *ACS Mater. Au* **2022**, *2*, 525−551.
(19) Hasan, J.; Crawford, R. J.; Ivanova, E. P. Antibacterial Surfaces: The Quest for a New Generation of Biomaterials. *Trends Biotechnol.* **2013**, *31*, 295−304.
(20) Suhardi, V.; Bichara, D.; Kwok, S.; Freiberg, A.; Rubash, H.; Malchau, H.; Yun, S.; Muratoglu, O.; Oral, E. A Fully Functional Drug-Eluting Joint Implant. *Nat. Biomed. Eng.* **2017**, *1*, 0080 DOI: 10.1038/s41551-017-0080.
(21) Kaur, R.; Liu, S. Antibacterial Surface Design−Contact Kill. *Prog. Surf. Sci.* **2016**, *91*, 136−153.
(22) Wang, Y.; Wang, F.; Zhang, H.; Yu, B.; Cong, H.; Shen, Y. Antibacterial Material Surfaces/Interfaces for Biomedical Applications. *Appl. Mater. Today* **2021**, *25*, No. 101192.
(23) Si, Z.; Zheng, W.; Prananty, D.; Li, J.; Koh, C. H.; Kang, E.-T.; Pethe, K.; Chan-Park, M. B. Polymers as Advanced Antibacterial and Antibiofilm Agents for Direct and Combination Therapies. *Chem. Sci.* **2022**, *13*, 345−364.
(24) Cuthbert, T. J.; Guterman, R.; Ragogna, P. J.; Gillies, E. R. Contact Active Antibacterial Phosphonium Coatings Cured with UV Light. *J. Mater. Chem. B* **2015**, *3*, 1474−1478.
(25) Cuthbert, T. J.; Harrison, T. D.; Ragogna, P. J.; Gillies, E. R. Synthesis, Properties, and Antibacterial Activity of Polyphosphonium Semi-Interpenetrating Networks. *J. Mater. Chem. B* **2016**, *4*, 4872−4883.
(26) Yu, Q.; Wu, Z.; Chen, H. Dual-Function Antibacterial Surfaces for Biomedical Applications. *Acta Biomater.* **2015**, *16*, 1−13.
(27) Zou, Y.; Zhang, Y.; Yu, Q.; Chen, H. Dual-Function Antibacterial Surfaces to Resist and Kill Bacteria: Painting a Picture with Two Brushes Simultaneously. *J. Mater. Sci. Technol.* **2021**, *70*, 24−38.
(28) Gevrek, T. N.; Yu, K.; Kizhakkedathu, J. N.; Sanyal, A. Thiol-Reactive Polymers for Titanium Interfaces: Fabrication of Antimicrobial Coatings. *ACS Appl. Polym. Mater.* **2019**, *1*, 1308−1316.
(29) Wei, T.; Yu, Q.; Chen, H. Responsive and Synergistic Antibacterial Coatings: Fighting against Bacteria in a Smart and Effective Way. *Adv. Healthcare Mater.* **2019**, *8*, No. 1801381, DOI: 10.1002/adhm.201801381.
(30) Li, X.; Wu, B.; Chen, H.; Nan, K.; Jin, Y.; Sun, L.; Wang, B. Recent Developments in Smart Antibacterial Surfaces to Inhibit Biofilm Formation and Bacterial Infections. *J. Mater. Chem. B* **2018**, *6*, 4274−4292.
(31) Wei, T.; Qu, Y.; Zou, Y.; Zhang, Y.; Yu, Q. Exploration of Smart Antibacterial Coatings for Practical Applications. *Curr. Opin. Chem. Eng.* **2021**, *34*, No. 100727.
(32) Sikder, A.; Chaudhuri, A.; Mondal, S.; Singh, N. P. Recent Advances on Stimuli-Responsive Combination Therapy against Multidrug-Resistant Bacteria and Biofilm. *ACS Appl. Bio Mater.* **2021**, *4*, 4667−4683.
(33) Wang, X.; Shan, M.; Zhang, S.; Chen, X.; Liu, W.; Chen, J.; Liu, X. Stimuli-Responsive Antibacterial Materials: Molecular Structures, Design Principles, and Biomedical Applications. *Adv. Sci.* **2022**, *9*, No. 2104843, DOI: 10.1002/advs.202104843.
(34) Xie, X.; Mao, C.; Liu, X.; Zhang, Y.; Cui, Z.; Yang, X.; Yeung, K. W.; Pan, H.; Chu, P. K.; Wu, S. Synergistic Bacteria Killing through Photodynamic and Physical Actions of Graphene Oxide/Ag/Collagen Coating. *ACS Appl. Mater. Interfaces* **2017**, *9*, 26417−26428.
(35) Mo, S.; Chen, X.; Chen, M.; He, C.; Lu, Y.; Zheng, N. Two-Dimensional Antibacterial Pd@ Ag Nanosheets with a Synergetic Effect of Plasmonic Heating and Ag^{+} Release. *J. Mater. Chem. B* **2015**, *3*, 6255−6260.
(36) Kwan, J. C.; Flannagan, R. S.; Vásquez Peña, M.; Heinrichs, D. E.; Holdsworth, D. W.; Gillies, E. R. Induction Heating Triggers Antibiotic Release and Synergistic Bacterial Killing on Polymer-Coated Titanium Surfaces. *Adv. Healthcare Mater.* **2023**, *12*, No. 2202807, DOI: 10.1002/adhm.202202807.
(37) Cado, G.; Aslam, R.; Séon, L.; Garnier, T.; Fabre, R.; Parat, A.; Chassepot, A.; Voegel, J. C.; Senger, B.; Schneider, F. Self-Defensive Biomaterial Coating against Bacteria and Yeasts: Polysaccharide Multilayer Film with Embedded Antimicrobial Peptide. *Adv. Funct. Mater.* **2013**, *23*, 4801−4809, DOI: 10.1002/adfm.201300416.
(38) Yao, Q.; Ye, Z.; Sun, L.; Jin, Y.; Xu, Q.; Yang, M.; Wang, Y.; Zhou, Y.; Ji, J.; Chen, H. Bacterial Infection Microenvironment-Responsive Enzymatically Degradable Multilayer Films for Multifunctional Antibacterial Properties. *J. Mater. Chem. B* **2017**, *5*, 8532−8541, DOI: 10.1039/C7TB02114C.
(39) Bjarnsholt, T.; Whiteley, M.; Rumbaugh, K. P.; Stewart, P. S.; Jensen, PØ.; Frimodt-Møller, N. The Importance of Understanding the Infectious Microenvironment. *Lancet Infect. Dis.* **2022**, *22*, e88−e92.
(40) Smith, S. M. D-Lactic Acid Production as a Monitor of the Effectiveness of Antimicrobial Agents. *Antimicrob. Agents Chemother.* **1991**, *35*, 237−241.
(41) Nalam, P. C.; Lee, H.-S.; Bhatt, N.; Carpick, R. W.; Eckmann, D. M.; Composto, R. J. Nanomechanics of pH-Responsive, Drug-Loaded, Bilayered Polymer Grafts. *ACS Appl. Mater. Interfaces* **2017**, *9*, 12936−12948.
(42) Pavlukhina, S.; Zhuk, I.; Mentbayeva, A.; Rautenberg, E.; Chang, W.; Yu, X.; Van De Belt-gritter, B.; Busscher, H. J.; Van der Mei, H. C.; Sukhishvili, S. A. Small-Molecule-Hosting Nanocomposite Films with Multiple Bacteria-Triggered Responses. *NPG Asia Mater.* **2014**, *6*, No. e121.
(43) Bu, Y.; Zhang, L.; Liu, J.; Zhang, L.; Li, T.; Shen, H.; Wang, X.; Yang, F.; Tang, P.; Wu, D. Synthesis and Properties of Hemostatic and Bacteria-Responsive in Situ Hydrogels for Emergency Treatment in Critical Situations. *ACS Appl. Mater. Interfaces* **2016**, *8*, 12674−12683.
(44) Dai, T.; Wang, C.; Wang, Y.; Xu, W.; Hu, J.; Cheng, Y. A Nanocomposite Hydrogel with Potent and Broad-Spectrum Antibacterial Activity. *ACS Appl. Mater. Interfaces* **2018**, *10*, 15163−15173.
(45) Phoungtawee, P.; Seidi, F.; Treetong, A.; Warin, C.; Klamchuen, A.; Crespy, D. Polymers with Hemiaminal Ether Linkages for pH-Responsive Antibacterial Materials. *ACS Macro Lett.* **2021**, *10*, 365−369.
(46) Wang, T.; Wang, C.; Zhou, S.; Xu, J.; Jiang, W.; Tan, L.; Fu, J. Nanovalves-Based Bacteria-Triggered, Self-Defensive Antibacterial Coating: Using Combination Therapy, Dual Stimuli-Responsiveness, and Multiple Release Modes for Treatment of Implant-Associated Infections. *Chem. Mater.* **2017**, *29*, 8325−8337.
(47) Li, S.; Zhao, S.; Pei, J.; Wang, H.; Meng, H.; Vrouwenvelder, J. S.; Li, Z. Stimuli-Responsive Lysozyme Nanocapsule Engineered Microfiltration Membranes with a Dual-Function of Anti-Adhesion and Antibacteria for Biofouling Mitigation. *ACS Appl. Mater. Interfaces* **2021**, *13*, 32205−32216.
(48) Ni, X.; Li, C.; Lei, Y.; Shao, Y.; Zhu, Y.; You, B. Design of a Smart Self-Healing Coating with Multiple-Responsive Superhydro-

phobicity and its Application in Antibiofouling and Antibacterial Abilities. *ACS Appl. Mater. Interfaces* **2021**, *13*, 57864−57879.
(49) Bradaric, C. J.; Downard, A.; Kennedy, C.; Robertson, A. J.; Zhou, Y. Industrial Preparation of Phosphonium Ionic Liquids. *Green Chem.* **2003**, *5*, 143−152.
(50) Harrison, T. D.; Ragogna, P. J.; Gillies, E. R. Phosphonium Hydrogels for Controlled Release of Ionic Cargo. *Chem. Commun.* **2018**, *54*, 11164−11167.
(51) Cuthbert, T. J.; Hisey, B.; Harrison, T. D.; Trant, J. F.; Gillies, E. R.; Ragogna, P. J. Surprising Antibacterial Activity and Selectivity of Hydrophilic Polyphosphoniums Featuring Sugar and Hydroxy Substituents. *Angew. Chem., Int. Ed.* **2018**, *57*, 12707−12710.
(52) Jain, R.; Standley, S. M.; Frechet, J. M. Synthesis and Degradation of pH-Sensitive Linear Poly(amidoamine)s. *Macromolecules* **2007**, *40*, 452−457.
(53) Hasan, A.; Saxena, V.; Pandey, L. M. Surface Functionalization of Ti6Al4V Via Self-Assembled Monolayers for Improved Protein Adsorption and Fibroblast Adhesion. *Langmuir* **2018**, *34*, 3494−3506.
(54) Pandey, L. M.; Pattanayek, S. K. Hybrid Surface from Self-Assembled Layer and its Effect on Protein Adsorption. *Appl. Surf. Sci.* **2011**, *257*, 4731−4737.
(55) Murata, H.; Koepsel, R. R.; Matyjaszewski, K.; Russell, A. J. Permanent, Non-Leaching Antibacterial Surfaces—2: How High Density Cationic Surfaces Kill Bacterial Cells. *Biomaterials* **2007**, *28*, 4870−4879.
(56) Gries, C. M.; Sadykov, M. R.; Bulock, L. L.; Chaudhari, S. S.; Thomas, V. C.; Bose, J. L.; Bayles, K. W. Potassium Uptake Modulates *Staphylococcus aureus* Metabolism. *mSphere* **2016**, *1*, No. e00125-16, DOI: 10.1128/mSphere.00125-16.
(57) Flannagan, R. S.; Heinrichs, D. E. A Fluorescence Based-Proliferation Assay for the Identification of Replicating Bacteria within Host Cells. *Front. Microbiol.* **2018**, *9*, No. 3084, DOI: 10.3389/fmicb.2018.03084.
(58) Harrison, T. D.; Yunyaeva, O.; Borecki, A.; Hopkins, C. C.; De Bruyn, J. R.; Ragogna, P. J.; Gillies, E. R. Phosphonium Polyelectrolyte Complexes for the Encapsulation and Slow Release of Ionic Cargo. *Biomacromolecules* **2020**, *21*, 152−162.
(59) Kanazawa, A.; Ikeda, T.; Endo, T. Novel Polycationic Biocides: Synthesis and Antibacterial Activity of Polymeric Phosphonium Salts. *J. Polym. Sci., Part A: Polym. Chem.* **1993**, *31*, 335−343.
(60) Kanazawa, A.; Ikeda, T.; Endo, T. Polymeric Phosphonium Salts as a Novel Class of Cationic Biocides. III. Immobilization of Phosphonium Salts by Surface Photografting and Antibacterial Activity of the Surface-Treated Polymer Films. *J. Polym. Sci., Part A: Polym. Chem.* **1993**, *31*, 1467−1472.
(61) Kanazawa, A.; Ikeda, T.; Endo, T. Polymeric Phosphonium Salts as a Novel Class of Cationic Biocides. X. Antibacterial Activity of Filters Incorporating Phosphonium Biocides. *J. Appl. Polym. Sci.* **1994**, *54*, 1305−1310.
(62) Wildemann, B.; Jandt, K. D. Infections@ Trauma/Orthopedic Implants: Recent Advances on Materials, Methods, and Microbes—a Mini-Review. *Materials* **2021**, *14*, 5834.
(63) Chopra, D.; Gulati, K.; Ivanovski, S. Understanding and Optimizing the Antibacterial Functions of Anodized Nano-Engineered Titanium Implants. *Acta Biomater.* **2021**, *127*, 80−101.
(64) Kugler, R.; Bouloussa, O.; Rondelez, F. Evidence of a Charge-Density Threshold for Optimum Efficiency of Biocidal Cationic Surfaces. *Microbiology* **2005**, *151*, 1341−1348.
(65) Shum, R. L.; Liu, S. R.; Caschera, A.; Foucher, D. A. UV-Curable Surface-Attached Antimicrobial Polymeric Onium Coatings: Designing Effective, Solvent-Resistant Coatings for Plastic Surfaces. *ACS Appl. Bio Mater.* **2020**, *3*, 4302−4315.
(66) Bedard, J.; Caschera, A.; Foucher, D. A. Access to Thermally Robust and Abrasion Resistant Antimicrobial Plastics: Synthesis of UV-Curable Phosphonium Small Molecule Coatings and Extrudable Additives. *RSC Adv.* **2021**, *11*, 5548−5555.
(67) Andersen, K. B.; von Meyenburg, K. Are Growth Rates of Escherichia Coli in Batch Cultures Limited by Respiration? *J. Bacteriol.* **1980**, *144*, 114−123.
(68) Kreevoy, M. M.; Taft, R. W., Jr. The Evaluation of Inductive and Resonance Effects on Reactivity. I. Hydrolysis Rates of Acetals of Non-Conjugated Aldehydes and Ketones1a. *J. Am. Chem. Soc.* **1955**, *77*, 5590−5595.
(69) Fife, T. H.; Anderson, E. Search for General Acid Catalysis of Acetal and Ketal Hydrolysis Reactions Based on Stability of the Intermediate Carbonium Ion. *J. Org. Chem.* **1971**, *36*, 2357−2361.
(70) Kanazawa, A.; Ikeda, T.; Endo, T. Polymeric Phosphonium Salts as a Novel Class of Cationic Biocides. Ii. Effects of Counter Anion and Molecular Weight on Antibacterial Activity of Polymeric Phosphonium Salts. *J. Polym. Sci., Part A: Polym. Chem.* **1993**, *31*, 1441−1447.
(71) Timofeeva, L.; Kleshcheva, N. Antimicrobial Polymers: Mechanism of Action, Factors of Activity, and Applications. *Appl. Microbiol. Biotechnol.* **2011**, *89*, 475−492.
(72) Król, J. E.; Hall, D. C.; Balashov, S.; Pastor, S.; Sibert, J.; McCaffrey, J.; Lang, S.; Ehrlich, R. L.; Earl, J.; Mell, J. C. Genome Rearrangements Induce Biofilm Formation in *Escherichia coli* C−An Old Model Organism with a New Application in Biofilm Research. *BMC Genomics* **2019**, *20*, No. 767, DOI: 10.1186/s12864-019-6165-4.
(73) Beloin, C.; Roux, A.; Ghigo, J. *Escherichia coli* Biofilms. *Curr. Top. Microbiol. Immunol.* **2008**, *322*, 249−289.
(74) Kenawy, E.-R.; Worley, S.; Broughton, R. The Chemistry and Applications of Antimicrobial Polymers: A State-of-the-Art Review. *Biomacromolecules* **2007**, *8*, 1359−1384.